Invited Review

Peptides as Models for the Structure and Function of Viral Capsid Proteins: Insights on Dengue Virus Capsid

João Miguel Freire,[1] Ana Salomé Veiga,[1] Beatriz G. de la Torre,[2] Nuno C. Santos,[1] David Andreu,[2] Andrea T. Da Poian,[3] Miguel A. R. B. Castanho[1]

[1]*Instituto de Medicina Molecular, Faculdade de Medicina, Universidade de Lisboa, Av. Prof. Egas Moniz, 1649-028 Lisbon, Portugal*

[2]*Department of Experimental and Health Sciences, Pompeu Fabra University, Barcelona Biomedical Research Park, E-08003 Barcelona, Spain*

[3]*Instituto de Bioquímica Médica, Universidade Federal do Rio de Janeiro, 21941-902 Rio de Janeiro, Brazil*

Received 16 March 2013; revised 11 April 2013; accepted 19 April 2013
Published online 19 July 2013 in Wiley Online Library (wileyonlinelibrary.com). DOI 10.1002/bip.22266

ABSTRACT:

The structural organization of viral particles is among the most astonishing examples of molecular self-assembly in nature, involving proteins, nucleic acids, and, sometimes, lipids. Proper assembly is essential to produce well structured infectious virions. A great variety of structural arrangements can be found in viral particles. Nucleocapsids, for instance, may display highly ordered geometric shapes or consist in macroscopically amorphous packs of the viral genome. Alphavirus and flavivirus are viral genera that exemplify these extreme cases, the former comprising viral particles structured with a $T = 4$ icosahedral symmetry, whereas flavivirus capsids have no regular geometry. Dengue virus is a member of flavivirus genus and is used in this article to illustrate how viral protein-derived peptides can be used advantageously over full-length proteins to unravel the foundations of viral supramolecular assemblies. Membrane- and viral RNA-binding data of capsid protein-derived dengue virus peptides are used to explain the amorphous organization of the viral capsid. Our results combine bioinformatic and spectroscopic approaches using two- or three-component peptide and/or nucleic acid and/or lipid systems. © 2013 Wiley Periodicals, Inc. Biopolymers (Pept Sci) 100: 325–336, 2013.

Keywords: flavivirus; dengue virus; nucleocapsid; viral peptides; nucleic acid interaction

Additional Supporting Information may be found in the online version of this article.

Correspondence to: Miguel A. R. B. Castanho, Instituto de Medicina Molecular, Faculdade de Medicina, Universidade de Lisboa, Av. Prof. Egas Moniz, 1649-028 Lisboa, Portugal; e-mail: macastanho@fm.ul.pt

Contract grant sponsor: Fundação para a Ciência e Tecnologia—Ministério da Educação e Ciência (FCT-MEC, Portugal)
Contract grant numbers: PTDC/QUI-BIQ/112929/2009; SFRH/BD/70423/2010
Contract grant sponsor: Fundação Calouste Gulbenkian
Contract grant sponsor: International Research Staff Exchange Scheme project MEMPEPACROSS (EU)
Contract grant numbers: FP7-PEOPLE IRSES; FP7-HEALTH-F3–2008-223414
Contract grant sponsor: Spanish Ministry of Economy and Competitivity
Contract grant number: SAF2011–24899
Contract grant sponsor: Conselho Nacional de Desenvolvimento Cientifico e Tecnologico (CNPq)
Contract grant number: 550114/2010-6
Contract grant sponsor: Fundação Carlos Chagas Filho de Amparo à Pesquisa do Estado do Rio de Janeiro (FAPERJ)
Contract grant number: E-26/102.919/2011
Contract grant sponsor: National Institute of Science and Technology in Dengue (INCT-Dengue)
Contract grant sponsor: Coordenação de Aperfeiçoamento de Pessoal de Nível Superior (CAPES, Brazil)
Contract grant number: PVE 171/2012

This article was originally published online as an accepted preprint. The "Published Online" date corresponds to the preprint version. You can request a copy of the preprint by emailing the Biopolymers editorial office at biopolymers@wiley.com

Viruses were discovered more than 100 years ago, and since then have been used as good models of simple, elegant, and functional supramolecular arrangements of proteins, nucleic acids, and, in some cases, lipid membranes. The incorporation of a replicon (functional genome) into a capsid (formed by numerous copies of capsid proteins) suffices to build a virion, a stable and infectious structure that is released from the host cell.[1–4] Some viruses also contain a lipid membrane that generally surrounds the nucleocapsid, forming what is called the viral envelope, which mediates viral infection through fusion with a cellular membrane. The challenge of achieving in-depth detail about the structural organization of the viral components, and the way they cooperate during viral infection contribute to the development of sophisticated high resolution techniques. These tools allowed great progress on the understanding of integrated biological systems and processes, such as lipid membrane dynamics and fusion,[5–11] as well as geometrical organization of protein structures.[5,9,12,13] These technological advances also pave the way for the discovery of new and more effective drugs against these pathogens,[14–17] specifically targeting crucial stages of the viral infection cycle.

Nevertheless, substantial challenges such as the menace of rising pandemics or the emergence of new strains/serotypes call for a relentless effort in updating our knowledge on virus structure and life cycle as an essential step toward developing novel and more potent therapies (vaccines or antiviral drugs) to fight these threats efficiently.[14,16–20]

Viruses from the *Flaviviridae* family cause important human diseases worldwide[20–23] and, among those, dengue virus (DENV) causes the major arthropod-borne human viral disease, which has significantly expanded in the last decades.[20,22–24] In this review, we revisit the unusual nongeometrical structure of the DENV capsid,[1,5,7,25,26] a feature shared with other viruses from this family, such as West Nile virus and tick-borne encephalitis virus. Data from the literature, supported by bioinformatics and biophysics data, are reinterpreted to provide new insights into the molecular structure of the DENV capsid, its role in the infectious process and eventually the establishment of new druggable viral targets.

DENGUE VIRUS: A HEALTH THREAT AND A SCIENTIFIC CHALLENGE

DENV causes the most important human arbovirosis (vector is primarily *Aedes aegypti*), with clinical manifestations that range from a self-limited fever to a very severe disease, which may progress to a fatal hypovolemic shock.[19,27,28] This clinical syndrome is a serious global health threat, responsible for over 20,000 deaths, with an estimation of 100 million people infected every year.[19,29–31] Transmission occurs mainly in tropical and subtropical regions[19,22,31,32]; however, due to climate changes, it is possible that this mosquito-borne illness may become emergent worldwide, with outbreaks in nontropical regions.[20,23,33]

Currently, no drug or vaccine to effectively treat or prevent DENV infection is available.[12,14,16,17,19,34–36] Extensive efforts have been carried out for vaccine development during the last 7 decades, and currently, some vaccines are under clinical trials.[20,24,34,36] In addition, apart from classical nonliving, attenuated, or chimeric DENV vaccines,[19–21] attempts to fight dengue also include antiviral strategies ranging from siRNA technology[27,28,37,38] to small molecules targeting DENV entering processes.[39–42] However, few of those initiatives have progressed beyond early preclinical studies. Regarding the DENV entry process as a potential druggable target, proteins that intervene during the membrane fusion and genome translocation into the host cell may serve as optimum candidates.[17,43] Despite the extensive background information on how DENV envelope (E) protein orchestrates viral-membrane interactions to achieve a successful infection, specific details are still lacking on whether additional viral proteins participate in this mechanism.[17,44]

Clearly, successful DENV control will require the joint efforts of vaccine and drug development research teams, as well as cross-disciplinary studies integrating structural, molecular, and cellular biology, and clinical areas.

NUCLEOCAPSID ASSEMBLY—INTERPLAY BETWEEN PROTEINS, NUCLEIC ACIDS, AND LIPIDS

Structurally, the capsids of nonenveloped viruses assume spherical or rod-like shapes. It was observed over the years that spherical viruses shared almost invariably icosahedral symmetry in their capsids.[4,13,46,47] However, for more complex, pleomorphic viruses (specifically those containing a lipid envelope), outliers to this symmetry arise and viruses may acquire or not a geometric nucleocapsid.[2,4] Generally, nucleocapsid formation may be interpreted as a well orchestrated molecular process involving protein–protein, protein–nucleic acid, and, eventually, protein–lipid interactions.[5,7,16,26,48,49] Thus, the landscape (broad or narrow) of allowed interactions between viral structural components may explain the formation of geometric and nongeometric nucleocapsids. As an example of the interplay between viral structural components to form a geometric particle, alphaviruses' (enveloped viruses) structure is paradigmatic (Figure 1). Envelope glycoproteins E1 and E2 form an icosahedral lattice with T = 4 symmetry. The C-terminal end of E2 interacts with the C-terminal end of the

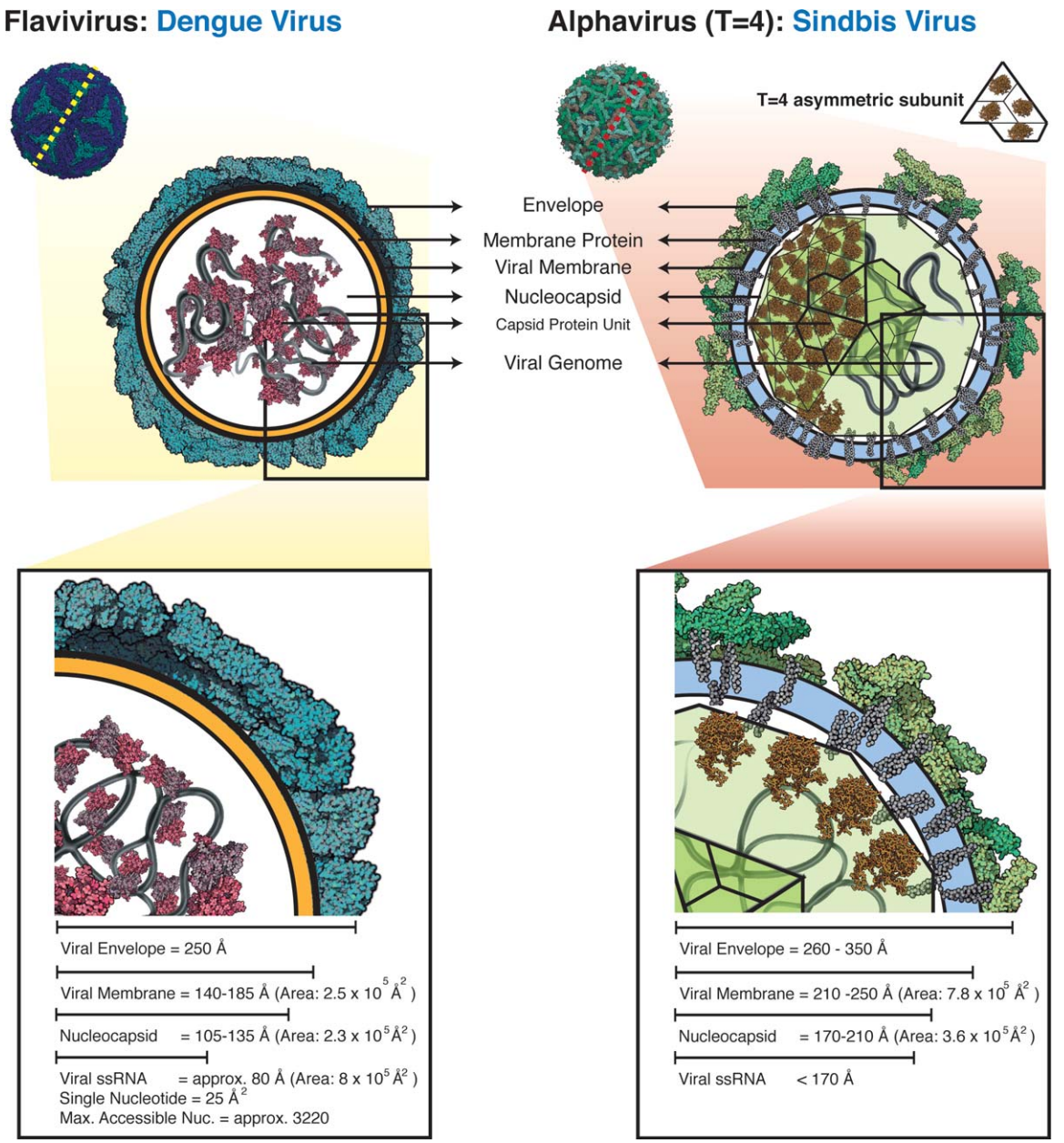

FIGURE 1 Structure of virions from flavivirus and alphavirus genera. General schematic representation of DENV[5,9] (flavivirus; left panel) and Sindbis virus (alphavirus; right panel).[50] The hypothetical DENV capsid arrangement and the radius of the both viral particles were obtained from the interpretation of the results shown in the Refs. 5 and 9 for DENV, and Ref. 50 for alphavirus. DENV and Sindbis virus structure ID were obtained from Viperdb (http://viperdb.scripps.edu),[51] ID: 1THD and ID: 1LD4, respectively.

capsid (C) protein, coordinating the assembly of the nucleocapsid that also shows T = 4 symmetry.[50,52,53]

For DENV, the viral particle (40–50 nm in diameter) consists in a lipoprotein envelope containing two associated structural proteins, membrane (M) and envelope (E). The envelope houses a ribonucleoprotein complex formed by capsid (C) protein bound to the positive-sense single-strand RNA (ssRNA) viral genome[1,54] (Figure 1). The ssRNA molecule is ~11 kb in length and has a single open reading frame that encodes, apart from the three structural proteins, seven nonstructural (NS) proteins (NS1, NS2A, NS2B, NS3, NS4A, NS4B, and NS5).[1,54]

DENV C protein forms a stable homodimer in solution (Figure 2A). Its sequence consists of 114 amino acid residues,

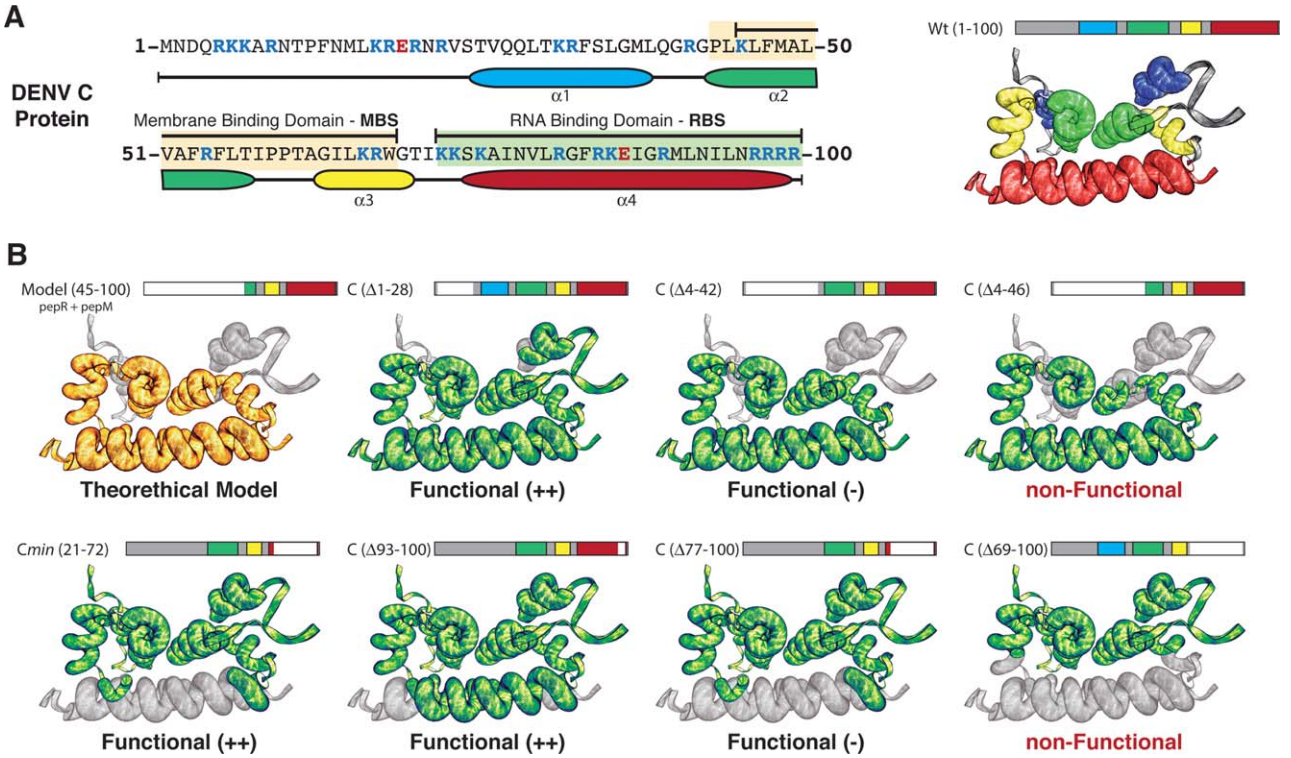

FIGURE 2 DENV C protein. A: Amino acid sequence of DENV C protein (from DENV serotype 2) with the identification of the α-helix regions (α_1—blue, α_2—green, α_3—yellow, α_4—red) (PDB: 1R6R).[21] B: Structure simulation of the functional and nonfunctional DENV C protein mutants based on the studies performed for the YFV C protein.[24] For the sake of simplicity, the maximum C- and N-terminal deletions tested for the YFV C protein that formed active or inactive virions[24] were extrapolated to simulate DENV C protein mutants. Three-dimensional structure alignment was performed in UCSF Chimera software[29] to validate the shared structural similarities between the C proteins from both viruses (Supporting Information Figure S1). The conformational representations were carried out with the PyMol software.[45]

which is reduced to 100 residues after release from the ER membrane.[1,21] It has 26 basic amino acid residues, with a global net charge of +46 (ProtParam[55]). Each monomer contains four α-helices (α1–α4) connected by short loops, and comprises two highly conserved internal regions: one hydrophobic and the other highly cationic.[21,56] NMR structure of DENV C protein revealed the charged and hydrophobic regions to be located at opposite faces of the protein[21,56] (Figure 2A). Based on charge distribution, it has been proposed that the C-terminal α4-α4′ region would bind viral RNA, whereas the hydrophobic core at the α2-α2′ region would be responsible for the interaction with lipids (viral and host) membranes.[1,21]

Despite a general knowledge on DENV proteomics, the complete structural organization of the virion, specifically regarding the nucleocapsid structure, is still unclear. Over the last decade, several cryoelectron microscopy studies of mature and immature DENV particles were performed,[5,7,9,26,57] mainly focusing on E protein rearrangements in the pre- and post-fusion conformations. However, these studies provided poor information about the capsid shell structure. Indeed, all the studied nucleocapsids of the members of *Flaviviridae* family were found to be amorphous and nongeometric.[5,7,26] In many situations, alphavirus and flavivirus biology (structural and molecular) was correlated due to the phylogenetic proximity of these families, and it was expected that flaviviruses would behave like alphaviruses.[13,58–60] However, contrary to what was observed for the T = 4 symmetry-nucleocapsids of alphaviruses, flaviviruses' nucleocapsids are poorly ordered. Such a fact might be explained by the lack of sufficient interaction points between nucleocapsid and membrane proteins to build stable anchor points for the icosahedron structure, as observed for alphaviruses.[50,52,53] In the next section, we hypothesize about the main aspects underlying the amorphous structure of flaviviruses' nucleocapsids, specifically focusing on the DENV capsid.

RNA Binding by Flaviviruses' C Proteins

Patkar et al. identified the minimal requirements of the dimeric C protein of yellow fever virus (YFV) for proper virion formation.[24] Several YFV C protein mutants containing N-, C-terminal, and internal deletions demonstrated a remarkable functional flexibility for this protein. Such data may contribute to clarify why flaviviruses' nucleocapsids are amorphous. Indeed, if a geometric capsid is considered, the modifications in the strict three-dimensional constraints of C protein necessary for proper capsid-nucleic acid and capsid-membrane interactions would hamper viral formation.

In the absence of a 3D structure for YFV C protein, and in order to evaluate whether the above findings by Patkar et al. could be applied to DENV C protein, a 3D structural model of YFV C protein was obtained by submitting its sequence to the I-TASSER web server,[39] which showed substantial structural homology between YFV and DENV C proteins (Supporting Information Section 1—Figure S1). The high sequence and structure homologies between DENV and YFV C proteins make it possible to simulate the hypothetical 3D structures of DENV C protein mutants resulting from amino acid deletions corresponding to those experimentally performed for YFV[24] (Figure 3 and Supporting Information Figure S1). Extrapolating from YFV to DENV, and applying the maximal C- and N-terminal deletions that in YFV C protein led to active virions, the biological viability of such DENV C mutants was theorized, indicating that deletions in the first 21 amino acid residues, as well as most of the α_4 domain would still result in infective virions (Figure 2B).

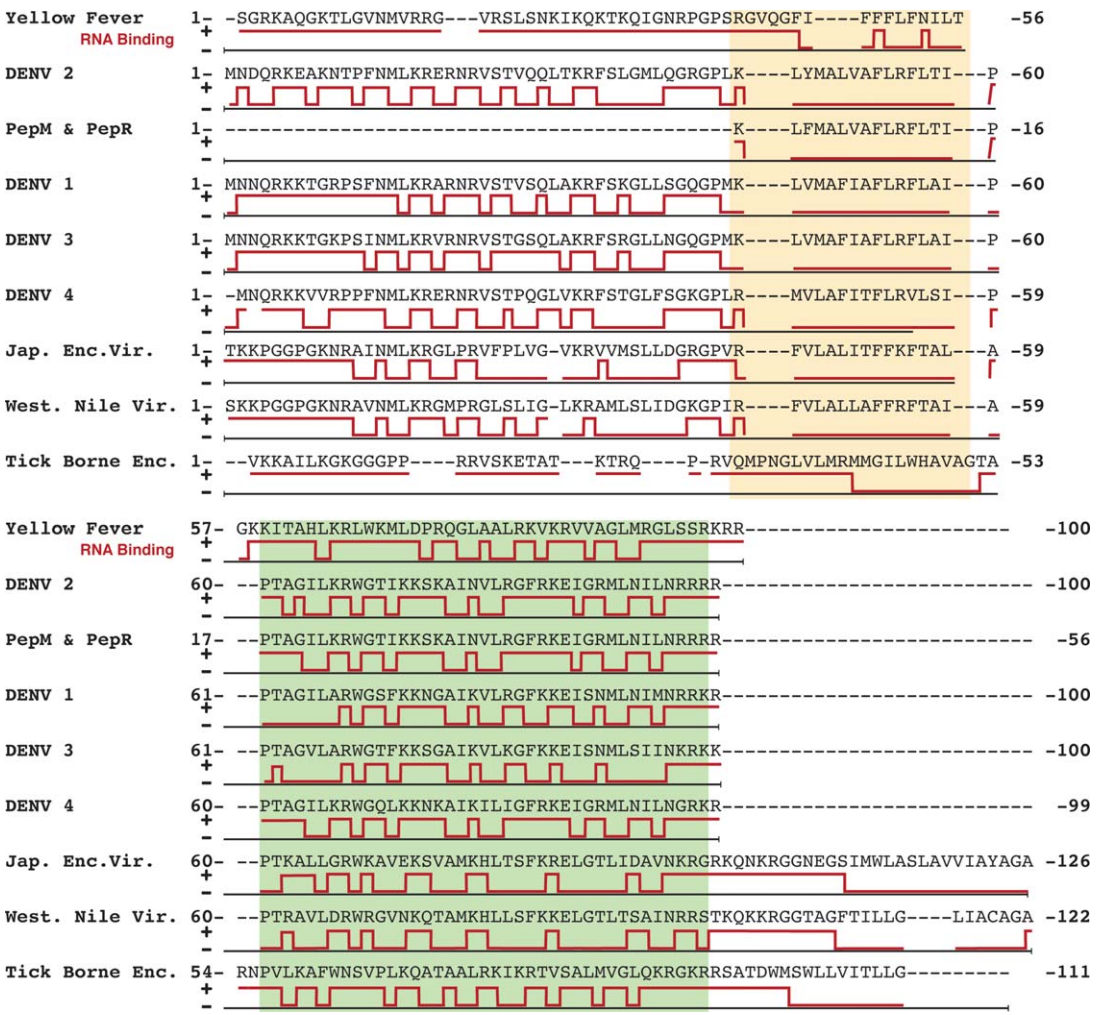

FIGURE 3 Sequence analysis of DENV and other flaviviruses' C proteins. Multiple protein sequence analyses of the flaviviruses' C proteins using Clustal Omega,[43] showing the respective RNA-binding propensity in each C protein sequence determined by RNABindR[32] (red line;- + and − correspond to positive and negative RNA binding residues, respectively). Highlighted yellow and green regions are assigned to the membrane- and RNA-binding domains, respectively.

To further explore the requirements for capsid assembly, we also determined the RNA binding propensity of flaviviruses' C proteins using the RNABindR web-tool,[32] which identifies putative sequences that specifically bind RNA (Figure 3). The N-terminal region of alphaviruses' C proteins has already been characterized as a specific RNA-binding segment.[12,16,61] Thus, the sequence of Sindbis virus (an alphavirus) C protein (264 amino acid residues) was submitted to RNABindR in order to validate the use of this tool to detect putative RNA-binding regions, i.e., domains in which the tendency to bind RNA is

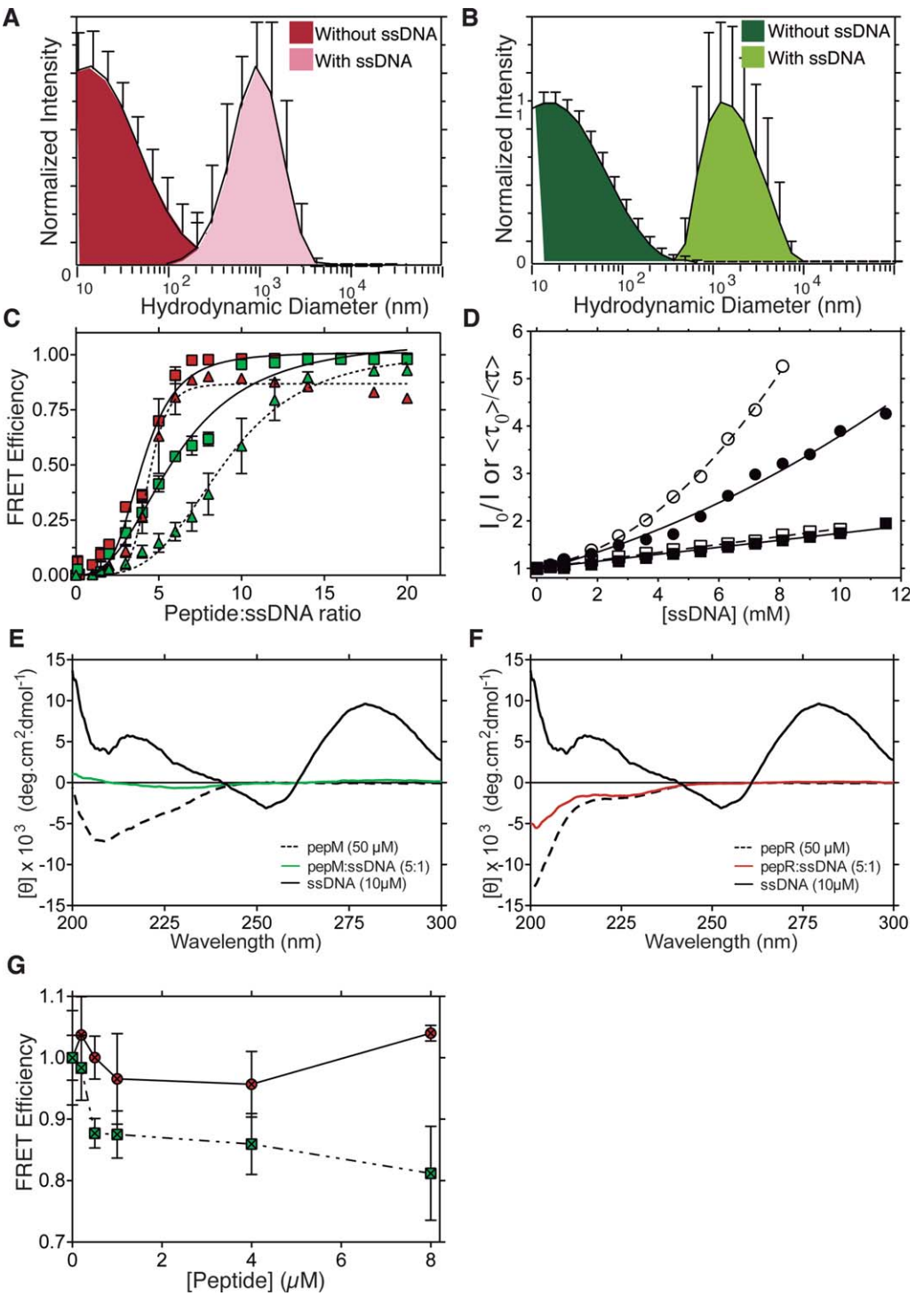

FIGURE 4

not merely due to unspecific electrostatics (Supporting Information Section 2—Figure S2). The first 110 amino acid residues of Sindbis C protein sequence were identified as a RNA-binding domain, supporting the use of this web-tool. For DENV C protein, sequence regions covered not only by α_4 but also by α_1 and α_3 regions showed high propensity to bind RNA, a result also observed for all flaviviruses' C proteins (Figure 3). Although it has been conjectured in the literature that the α_4 region would be the RNA-binding domain in DENV,[1,21] RNABindR data suggests that all flavivirus' C protein sequence is prone to bind RNA; no specific RNA-binding domains within flaviviruses' C proteins could be identified or assigned. These results, especially those obtained for YFV, would explain the above findings for YFV C protein mutants that can encapsulate YFV genome and produce infective particles even after extensive deletions.[24] Additionally, the promiscuity of RNA binding propensity throughout all flaviviruses' C proteins may explain the amorphous nucleocapsid structure of these viruses, in contrast with the view that DENV C protein contains functionally distinct domains, the α_2-α_3 assigned to membrane binding and the α_4 assigned to RNA-binding.[1,21] Rather, our study supports the hypothesis that the full length DENV C protein could function as the N-terminal regions of alphaviruses.[7]

PEPTIDES AS MODELS FOR CAPSID PROTEINS

Synthetic peptide replicas have been extensively used to characterize and identify the biological functions of protein domains.[24,62] Several in vitro and theoretical approaches have been also used to highlight important regions of capsid proteins and viral genomes for the proper assembly of the nucleocapsid structure.[14,24,48,49,63–65] DENV nucleocapsid assembly studies have yet not been reported in the literature, raising the possibility of using peptides to study the functional elements of the DENV C protein responsible for RNA-binding and nucleocapsid assembly.

Insights on DENV Capsid Structure and Dynamics From Selected Model Peptides

To have an insight on DENV nucleocapsid structure and assembly, we conducted protein–nucleic acid and protein–membrane interaction studies using two synthetic peptides predicted as putative C protein membrane- and RNA-binding domains[21,56]: pepM and pepR, respectively. If restrictive structural constraints were required for DENV nucleocapsid formation, only one of the domains, pepR, would strongly interact with nucleic acids, whereas pepM would have no significant affinity and would in principle prefer hydrophobic lipid environments. Conversely, an amorphous DENV nucleocapsid showing no regular structural pattern would be compatible with both regions revealing similar affinity to nucleic acids, as suggested by the above DENV C protein mutant predictions and RNABindR data (Figures 2B and 3, respectively).

A 15-nucleotide ssDNA molecule, as previously validated by Kiermayr et al.[63] for nucleocapsid formation studies, was used as nucleic acid model in binding experiments with pepM and pepR. ssDNA avoids experimental limitations when using RNA, such as nucleic acid degradation by environmental RNases. Using DNA molecules, proper core-like particles have already been produced for alphaviruses' C proteins,[63] which exhibited a sedimentation behavior in sucrose gradients similar to viral capsids isolated from virions. Peptide-nucleic acids binding was assessed by dynamic light scattering (DLS), Förster resonance energy transfer (FRET), circular dichroism (CD), and fluorescence readouts (Figure 4). DLS results revealed that both pepR and pepM (Figures 4A and 4B, respectively) form peptide-ssDNA complexes, because particle

FIGURE 4 Interaction of DENV C protein domains with nucleic acids. A and B: Normalized size distribution histograms corresponding to hydrodynamic diameters obtained by dynamic light scattering spectroscopy for 100 μM pepR (A) or pepM (B) in the presence of ssDNA at a peptide:ssDNA ratio of 2.5:1 (pepR) or 5:1 (pepM). Significant size distribution changes are observed after the titration with ssDNA. Error bars show the SD of 3 independent experiments. C: Association curves between ssDNA and DENV C protein-derived peptides, pepR (red) and pepM (green), determined by FRET at pH 7.4 (squares) and 5.5 (triangles). Binding constants were determined using Eq. (3) from the "Materials and Methods" section. D: Stern–Volmer plots of 36 μM pepR (squares) or pepM (circles) after titration with ssDNA (0 to 12 μM) at pH 7.4 (filled symbols) or 5.5 (empty symbols). Equations (7) and (12) were used to fit data of pepM and pepR, respectively. E and F: CD spectra of 10 μM of ssDNA (solid line); 50 μM of pepM (E) and pepR (F) in buffer (dashed line), and in the presence of 10 μM of ssDNA (green-pepM and red-pepR lines). G: DENV C protein-derived peptides competition assay for ssDNA binding. A solution of 2 μM ssDNA-Alexa488 previously incubated with 26 μM of either pepR (red) or pepM (green) labeled with Rhodamine B was titrated with up to 8 μM nonlabeled pepM or pepR, respectively. FRET efficiencies of the Alexa488/Rhodamine B pairs were quantified.

Table I Binding Constants of Both DENV C Protein-Derived Peptides to Nucleic Acids, Determined by Fluorescence Quenching ($K_{d,\ app}$) or FRET (K_d and Stoichiometry)

		pepR	pepM	$K_{D\ (pepR)}/K_{D\ (pepM)}$
Quenching	pH 7.4	13.7 ± 0.2	16.1 ± 4.0	0.85
$1/K_{SV}$ ($K_{d,\ app}$) (μM)	pH 5.5	11.9 ± 2.3	23.2 ± 7.1	0.52
	Equation	(7)	(7)	
FRET	pH 7.4	4.02 ± 0.10 (3.9 ± 0.3)	6.04 ± 0.27 (2.5 ± 0.2)	0.66
K_d (μM) (Stoichiometry)	pH 5.5	4.38 ± 0.10 (7.7 ± 1.2)	8.98 ± 0.43 (3.6 ± 0.3)	0.49
	Equation	(3)	(3)	

size in the presence of ssDNA increased by a similar extent for both peptides. The dissociation constant (K_d) and the binding stoichiometry obtained by FRET experiments (Figure 4C), together with the apparent binding constants ($K_{d,\ app}$) obtained from fluorescence quenching experiments (Figure 4D), also suggested very similar binding properties for pepR and pepM (Table I). This is in agreement with the RNABindR analyses that showed RNA-binding segments along all the DENV C protein sequence (Figure 3). Additionally, the prediction of functional C proteins despite deletions in either most of pepM or pepR sequences (Figure 2) is also consistent with both regions having similar affinity for nucleic acids. CD spectroscopy, concomitantly, showed a decrease in the intensity of both DNA and peptide signatures on mixing (Figures 4E and 4F), indicating that both pepR and pepM form supramolecular complexes in the presence of the oligonucleotides.[66,67] To evaluate stability, pepR-ssDNA or pepM-ssDNA complexes made with a fluorescently labeled version of either peptide were titrated with unlabeled pepM or pepR, respectively. In this assay, a drop in FRET efficiency indicates that the unlabeled peptide is competing for the ssDNA molecules bound to the labeled peptide. As shown in Figure 4G, pepR-ssDNA complexes are not as perturbed by pepM addition as vice versa, suggesting that pepR forms slightly more stable complexes with oligonucleotides than pepM, in agreement with the binding constants in Table I. However, in neither of the two situations disruption of pre-formed peptide-ssDNA complexes could be judged as drastic. These data altogether lead us to propose a model in which the whole DENV C protein (pepM and pepR—Figure 2B yellow model) would nonspecifically bind the DENV genome, through a histone/chromatin-like interaction, to assembly an amorphous and compact nucleocapsid core (Figure 5), lacking membrane anchoring points. In fact, to form a geometrical capsid, each C protein would need to be perfectly oriented within the viral core, having stable protein-RNA on one side and stable protein–membrane interactions on the opposing side, such as in alphaviruses.[12,16,61] For a small-size building block as DENV C protein is,[5,7,26] with no well-defined domains for binding to the viral genome and for anchoring in the membrane, a geometrical capsid formation would not be favored. The simplest geometric supramolecular arrangement, a T = 3 symmetry capsid, would require 120 DENV C protein dimers exposed to the membrane, but 400 of such dimers would be required to bind the RNA coil surface (Supporting Information Section 3—Figures S3 and S4). This mismatch reinforces the idea of a compact and amorphous ribonucleoprotein core.

CONCLUDING REMARKS

Viral self-assembly occurs within the cell, where hundreds of individual capsid protein subunits must recognize and specifically package the viral components within an environment characterized by an immense molecular crowding. Viral capsid proteins are also involved in other stages of the virus life cycle,[2] which may imply that these proteins retain some intrinsic flexibility upon cellular infection, which contrasts with their stability within the virion. There have been several attempts to explain the physico-chemical properties and thermodynamic stability of viral capsids and their assembly[68–70]; however, few examples are suitable or directly relatable to flaviviruses.

Here, we reviewed the previous observations that DENV nucleocapsid structure is disordered rather than geometric, and further supported this view with original bioinformatics simulations as well as biophysics studies using viral protein-derived peptides. The data presented here show no striking differences between pepR and pepM in their binding to nucleic acids, suggesting that the model of DENV C protein having specific regions assigned to different functions (membrane- and viral RNA-binding)[1,21] needs to be revisited. Additionally, we hypothesize that the promiscuity of DENV C protein sequence regions in binding RNA or membranes contributes to the previously observed amorphous nucleocapsid.[5,7,26] This also supports why the extensive deletions in

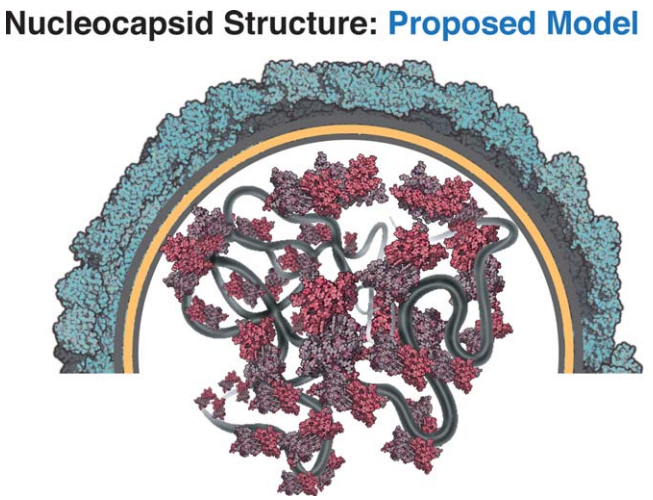

FIGURE 5 Interpretation of DENV C protein-ssRNA packing and viral assembly. A T = 3-like DENV capsid was hypothesized but a geometrical analysis reveals its inconsistency: the capsid would have 1162 Å^2, which would accommodate nearly 120 protein C dimers, contrasting with the 180 proteins needed for a T = 3 capsid. Moreover, such capsid would imply that only a specific domain would be available to interact with RNA and, therefore, 430 dimers would be required for complete RNA stabilization. A histone-like packing is proposed, which implies that ~143 dimers suffice to stabilize the capsid. DENV C protein dimer size was obtained by PyMol[45] software (using PDB ID: IR6R)[21] (Supporting Information Figure S3).

YFV C protein sequence,[24] and probably in DENV C protein as well (as hypothesized in Figure 2), do not affect significantly virion production, as the remaining C protein sequence would be able to interact with viral RNA during assembly. In this context, the suggestion that DENV C protein would function as the N-terminal region of alphaviruses' C proteins[7,26] is plausible. However, one should bear in mind that no sequence or structural homology between the N-terminal regions of DENV and alphaviruses' C proteins has been observed (Supporting Information Figure S2).

It is interesting to note that almost all C proteins that form capsids with icosahedral symmetry share a remarkable convergence of folding patterns.[2,71] However, for flaviviruses' C proteins such structural homology does not occur and examples of nonicosahedral nucleocapsids abound.

Viruses are entities in which protein, nucleic acid, and lipid are arranged in an integrated way. When a key module of this structure, such as the capsid, is lost, no infectious virions can be formed. Thus, gaining structural information on virion architecture should enable a deeper understanding of these cellular parasites. Because nucleocapsid assembly is one of the most crucial steps in producing infectious viruses, understanding this key process in the DENV replication cycle may reveal new approaches to fight and prevent the severe disease caused by DENV, as well as those related to other flaviviruses.

MATERIALS AND METHODS

Chemicals

Fmoc-protected amino acids were obtained from Senn Chemicals (Dielsdorf, Switzerland) and Fmoc-Rink-amide (MBHA) resin from Novabiochem (Läufelfingen, Switzerland). 2-(1H-benzotriazol-1-yl)−1,1,3,3-tetramethyluronium hexafluorophosphate and *N*-hydroxybenzotriazole were from PCAS Biomatrix (Saint Jean sur Richelieu, Quebec, Canada). HPLC-grade acetonitrile, and peptide synthesis-grade *N*,*N*-dimethylformamide, dichloromethane, *N*,*N*-diisopropylethylamine, and trifluoroacetic acid were from Carlo Erba-SDS (Sabadell, Spain). The ssDNA (ACG TGC TGA GCC TAC) and ssDNA-Alexa488 were obtained from Molecular Probes/Invitrogen (Life Technologies, Carlsbad, CA). 4-(2-Hydroxyethyl)−1-piperazineethanesulfonic acid (HEPES) and NaCl were acquired from Sigma-Aldrich (St. Louis, MO). L-Tryptophan was from Merck (Darmstadt, Germany). All other reagents were of the highest quality available commercially. All experiments were performed using 10 m*M* HEPES buffer pH 7.4 in NaCl 150 m*M*, if not otherwise stated.

Flaviviruses' Capsid Proteins Computational Analysis

The three-dimensional molecular visualizer PyMol (v1.4)[45] was used to represent DENV (PDB: 1R6R[21]) and Sindbis virus (PDB: 1SVP[72]) C proteins. Flaviviruses' and alphaviruses' C proteins multiple alignment were obtained by Clustal Omega (EBI)[43] (http://www.ebi.ac.uk/Tools/msa/clustalo/). Additionally, for each flavivirus and for Sindbis virus (an alphavirus) C protein sequence, high-RNA affinity domains were predicted by the web-tool RNABindR[32] (http://einstein.cs.iastate.edu/RNABindR/).

DENV C Protein Domain Models—pepM and pepR

Both pepM (KLFMALVAFLRFLTIPPTAGILKRWGTI—residues 45–72 of C protein from DENV serotype 2, DENV-2) and pepR (LKRWGTIKKSKAINVLRGFRKEIGRMLNILNRRRR—residues 67–100 of DENV-2 C protein), as well as their N-terminal Rhodamine B-labeled versions, were prepared by solid phase synthesis methods, as previously described[73,74] (detailed description on synthesis as well as the MALDI-TOF and HPLC spectra from the purification steps available in Ref. 74). pepR, pepM, and their respective fluorescent derivatives stock solutions were prepared in Milli Q Water.

Interaction of DENV C Protein Domains With Nucleic Acids

The complexation between DENV C protein specific domains (pepM and pepR) and oligonucleotides was studied by FRET, DLS, CD, and fluorescence quenching. FRET and quenching studies report peptide-ssDNA association at the molecular level, DLS reports the formation of mixed peptide-ssDNA supramolecular aggregates, while CD screens for structural rearrangements of these high-order molecular aggregates.

Förster Resonance Energy Transfer. In FRET experiments, a 2 μ*M* ssDNA-Alexa488 solution was titrated with up to 26 μ*M* of either pepR or pepM labeled with Rhodamine-B. Samples were excited at

492 nm; emission spectra were collected from 500 to 700 nm and blank corrected. Steady-state fluorescence spectra were collected in a FS920 fluorescence spectrophotometer (Edinburgh Instruments, Livingston, UK), equipped with two double monochromators and a 750 W xenon lamp. The assay was performed at both pH 7.4 and 5.5 (using a 10 m*M* citrate buffer, 150 m*M* NaCl). FRET efficiency was calculated according to[75,76]:

$$\text{FRET Efficiency} = 1 - \frac{I_i}{I_0}, \quad (1)$$

where I_i and I_0 are the ratios of the fluorescence intensity (at maximum emission wavelength) between the donor and the acceptor fluorophores at the i concentration of peptide and donor spectra (ssDNA-Alexa488) in buffer, respectively. The detailed formalism is described elsewhere.[76] FRET data were interpreted using an ssDNA-peptide Hill binding curve model. Assuming that the interaction of both molecules is described by the equilibrium:

$$n(peptide) + ssDNA \rightleftarrows peptide_n ssDNA$$

The dissociation constant, K_d, is given by:

$$K_d = \frac{[peptide]^n [ssDNA]}{[peptide_n ssDNA]}, \quad (2)$$

Considering that pepR or pepM are interacting with the ssDNA molecule in a stoichiometry n, with a well-defined average donor–acceptor distance, the extent of the supramolecular complex formation can be directly correlated with the average efficiency of the FRET process. FRET efficiency data were fitted using the Hill binding equation, in order to determine the dissociation constant, K_d, and the stoichiometry of the reaction, n:

$$FRET\ efficiency = \frac{Max_{binding}[peptide]^n}{K_d^n + [peptide]^n}, \quad (3)$$

The empirical percent binding was calculated from the ratio of the FRET efficiency to FRET efficiency at maximal binding:

$$\%Binding = \left(\frac{FRET\ Efficiency}{FRET\ Efficiency_{MaxBinding}}\right) \times 100\%, \quad (4)$$

Dynamic Light Scattering. DLS experiments were carried out on a Malvern Zetasizer Nano ZS (Malvern, UK) with backscattering detection at 173°, equipped with a He–Ne laser ($\lambda = 632.8$ nm), at 25°C (15 min of equilibration). Measurements were performed in 100 μ*M* solutions of pepR and pepM in the absence and in the presence of the ssDNA oligonucleotide, at peptide:ssDNA molar ratios of 5:2 (pepR) or 5:1 (pepM). For each sample, the instrument was set to perform 15 scans, each one giving an autocorrelation curve after at least 70 measurements, with an initial equilibration time of 15 min at 25°C. Normalized intensity autocorrelation function, average of the 15 obtained, was analyzed using the CONTIN method,[77,78] retrieving a distribution of diffusion coefficients (D), which can be used for the calculation of the scattering particles' hydrodynamic diameter (D_H)[79,80] distribution through the Stokes-Einstein (Eq. (5)):

$$D = \frac{kT}{3\pi\eta D_H}, \quad (5)$$

where k is the Boltzmann constant, T is the absolute temperature, and η is the medium viscosity. The D_H of the sample was considered from the peak with the highest scattered light intensity (i.e., the mode) in light scattering intensity distributions.

Circular Dichroism. CD spectra of 50 μ*M* pepR or pepM in buffer (HEPES 10 m*M*, 50 m*M* NaF, pH 7.4), in the absence or presence of 10 μ*M* ssDNA, were acquired at 25°C, in the 195–300 nm wavelength range, using 0.1 cm quartz cells, in a JASCO spectropolarimeter model J-815 (Tokyo, Japan). Each final spectrum corresponds to the average of 10 runs, which were subsequently corrected for buffer or LUV baselines. The obtained spectra were represented as a function of mean residue molar ellipticity, $[\theta]$,[81] according to the equation:

$$[\theta] = \frac{\varepsilon}{aa \times l \times c}, \quad (6)$$

where ε is the observed ellipticity, aa is the number of amino acid residues in the peptide sequence, l is the quartz cell path length, and c is the peptide concentration. The pepR and pepM's contents of standard secondary structure elements were assessed using the web-tool software K2D3 (http://www.ogic.ca/projects/k2d3//index.html).[82]

Fluorescence Quenching. The interaction of either pepR or pepM with oligonucleotides was studied using the Trp fluorescence quenching caused by the contact with the nucleic acid.[83] When a fluorescence quenching process has a static component, this refers to the ground-state complexation of fluorophore (the peptides, in this case) and quencher (ssDNA). If both dynamic (collisional) and static (complexation) components are present, the Stern-Volmer formalism is:

$$\frac{I_0(t)}{I(t)} = (1 + K_s[Q]) \times (1 + K_D[Q]), \quad (7)$$

where K_S and K_D are the static and dynamic Stern-Volmer constants, respectively. K_S is an apparent fluorophore-quencher (peptide-ssDNA) binding constant.[75] To calculate K_S, K_D has to be known. Time resolved fluorescence spectroscopy was used with the purpose of calculating both K_S and K_D.

A 36 μ*M* solution of pepR or pepM was titrated with ssDNA (up to 12 μ*M*) at both pH 7.4 (10 m*M* HEPES, 150 m*M* NaCl) and pH 5.5 (10 m*M* citrate buffer, 150 m*M* NaCl). Time-resolved fluorescence emission decays were performed in a LifeSpec II apparatus (Edinburgh Instruments, Livingston, UK), equipped with an Epled-280 (laser of 275 nm with a repeating rate of 200 ns). Fluorescence emission was collected at 350 nm (emission slits of 23 nm). A 20 ns range was used for decay acquisition, divided in 2048 channels. Signal acquisition duration was set to 20 min. Instrumental response functions were generated from scatter dispersion (glycogen solution, Acros Organics, Geel, Belgium). FAST software was used for data analysis using a nonlinear least-squares iterative convolution method (Edinburgh Instruments). Fluorescence decays were analyzed using:

$$I(t) = \sum \alpha_i e^{\frac{-t}{\tau_i}}, \quad (8)$$

where α_i is the pre-exponential factor in a multiexponential intensity decay, t is time, and τ_i is the ith component excited state fluorescence lifetime.[75,84] The goodness of the fit was evaluated from the residual distributions and the χ^2 value (decay fits with $0.99 < \chi^2 < 1.1$ were accepted).

The Trp fluorescence decay was fitted by a sum of three exponentials[84] and the average lifetime, $<\tau>$, was determined according to:

$$\langle\tau\rangle = \frac{\sum \alpha_i \tau_i^2}{\sum \alpha_i \tau_i}, \tag{9}$$

The Stern-Volmer quenching formalism can be applied to time resolved data as $I_0/I = <\tau>_0/<\tau>$.[75,84] The Stern-Volmer constant in this case refers only to dynamic (collisional) phenomenon, K_D:

$$\frac{\langle\tau\rangle_0}{\langle\tau\rangle} = 1 + K_D[Q], \tag{10}$$

The decays integral is related to the total fluorescence emission intensity of the fluorophore during the acquisition time. Because the acquisition time was kept constant throughout the experiments (20 min),

$$\frac{\int_t I_0(t)}{\int_t I(t)} = \frac{I_0}{I}, \tag{11}$$

K_S was determined using Eq. (7) with the K_D previously determined from Eq. (10), in the case of both static and collisional quenching occurring simultaneously. For the Stern-Volmer formalism:

$$\frac{\int_t I_0(t)}{\int_t I(t)} = 1 + K_{SV}[Q], \tag{12}$$

REFERENCES

1. Mukhopadhyay, S.; Kuhn, R. J.; Rossmann, M. G. Nat Rev Microbiol 2005, 3, 13–22.
2. Abrescia, N. G. A.; Bamford, D. H.; Grimes, J. M.; Stuart, D. I. Annu Rev Biochem 2012, 81, 795–822.
3. Vancini, R.; Kramer, L. D.; Ribeiro, M.; Hernandez, R.; Brown, D. Virology 2013, 435, 406–414.
4. Veesler, D.; Johnson, J. E. Annu Rev Biophys 2012, 41, 473–496.
5. Kuhn, R. J.; Zhang, W.; Rossmann, M. G.; Pletnev, S. V.; Corver, J.; Lenches, E.; Jones, C. T.; Mukhopadhyay, S.; Chipman, P. R.; Strauss, E. G.; Baker, T. S.; Strauss, J. H. Cell 2002, 108, 717–725.
6. Harrison, S. C. Nat Struct Mol Biol 2008, 15, 690–698.
7. Zhang, Y.; Corver, J.; Chipman, P. R.; Zhang, W.; Pletnev, S. V.; Sedlak, D.; Baker, T. S.; Strauss, J. H.; Kuhn, R. J.; Rossmann, M. G. EMBO J 2003, 22, 2604–2613.
8. Kielian, M.; Rey, F. A. Nat Rev Microbiol 2006, 4, 67–76.
9. Zhang, X.; Ge, P.; Yu, X.; Brannan, J. M.; Bi, G.; Zhang, Q.; Schein, S.; Zhou, Z. H. Nat Struct Mol Biol 2012, 20, 105–110.
10. Chernomordik, L. V.; Kozlov, M. M. Nat Struct Mol Biol 2008, 15, 675–683.
11. Chernomordik, L. V.; Zimmerberg, J.; Kozlov, M. M. J Cell Biol 2006, 175, 201–207.
12. Frolova, E.; Frolov, I.; Schlesinger, S. J Virol 1997, 71, 248–258.
13. Rossmann, M. G.; Johnson, J. E. Annu Rev Biochem 1989, 58, 533–569.
14. Perera, R.; Owen, K. E.; Tellinghuisen, T. L.; Gorbalenya, A. E.; Kuhn, R. J. J Virol 2001, 75, 1–10.
15. Bollati, M.; Alvarez, K.; Assenberg, R.; Baronti, C.; Canard, B.; Cook, S.; Coutard, B.; Decroly, E.; de Lamballerie, X.; Gould, E. A.; Grard, G.; Grimes, J. M.; Hilgenfeld, R.; Jansson, A. M.; Malet, H.; Mancini, E. J.; Mastrangelo, E.; Mattevi, A.; Milani, M.; Moureau, G.; Neyts, J.; Owens, R. J.; Ren, J.; Selisko, B.; Speroni, S.; Steuber, H.; Stuart, D. I.; Unge, T.; Bolognesi, M. Antivir Res 2010, 87, 125–148.
16. Hong, E. M.; Perera, R.; Kuhn, R. J. J Virol 2006, 80, 8848–8855.
17. Pierson, T. C.; Kielian, M. Curr Opin Virol 2013, 3, 3–12.
18. Kasson, P. M.; Pande, V. S. Proc Natl Acad Sci USA 2011, 108, 3827–3828.
19. Murphy, B. R.; Whitehead, S. S. Annu Rev Immunol 2011, 29, 587–619.
20. Laughlin, C. A.; Morens, D. M.; Cassetti, M. C.; Costero-Saint Denis, A.; San Martin, J. L.; Whitehead, S. S.; Fauci, A. S. J Infect Dis 2012, 206, 1121–1127.
21. Ma, L.; Jones, C. T.; Groesch, T. D.; Kuhn, R. J.; Post, C. B. Proc Natl Acad Sci USA 2004, 101, 3414–3419.
22. Guzmán, M. G.; Halstead, S. B.; Artsob, H.; Buchy, P.; Farrar, J.; Gubler, D. J.; Hunsperger, E.; Kroeger, A.; Margolis, H. S.; Martínez, E. Nat Rev Microbiol 2010, 8, S7–S16.
23. Lindgren, E.; Andersson, Y.; Suk, J. E.; Sudre, B.; Semenza, J. C. Science 2012, 336, 418–419.
24. Patkar, C. G.; Jones, C. T.; Chang, Y. H.; Warrier, R.; Kuhn, R. J. J Virol 2007, 81, 6471–6481.
25. Gebhard, L. G.; Filomatori, C. V.; Gamarnik, A. V. Viruses 2011, 3, 1739–1756.
26. Zhang, W.; Chipman, P. R.; Corver, J.; Johnson, P. R.; Zhang, Y.; Mukhopadhyay, S.; Baker, T. S.; Strauss, J. H.; Rossmann, M. G.; Kuhn, R. J. Nat Struct Biol 2003, 10, 907–912.
27. Owen, K. E.; Kuhn, R. J. J Virol 1996, 70, 2757–2763.
28. Owen, K. E.; Kuhn, R. J. Virology 1997, 230, 187–196.
29. Pettersen, E. F.; Goddard, T. D.; Huang, C. C.; Couch, G. S.; Greenblatt, D. M.; Meng, E. C.; Ferrin, T. E. J Comput Chem 2004, 25, 1605–1612.
30. Beatty, M. E.; Stone, A.; Fitzsimons, D. W.; Hanna, J. N.; Lam, S. K.; Vong, S.; Guzmán, M. G.; Mendez-Galvan, J. F.; Halstead, S. B.; Letson, G. W.; Kuritsky, J.; Mahoney, R.; Margolis, H. S.; for The Asia-Pacific and Americas Dengue Prevention Boards Surveillance Working Group. PLoS Negl Trop Dis 2010, 4(11), e890 (7 pp).
31. World Health Organization. Dengue and Severe Dengue. January 20, 2012. Available at: http://www.who.int/mediacentre/factsheets/fs117/en/.
32. Terribilini, M.; Sander, J. D.; Lee, J. H.; Zaback, P.; Jernigan, R. L.; Honavar, V.; Dobbs, D. Nucleic Acids Res 2007, 35, W578–W584.

33. Sousa, C.; Clairouin, M.; Seixas, G.; Viveiros, B.; Novo, M.; Silva, A.; Escoval, M.; Economopoulou, A. Euro Surveill 2012, 17(49) (4 pp).
34. Webster, D. P.; Farrar, J.; Rowland-Jones, S. Lancet Infect Dis 2009, 9, 678–687.
35. Wilder-Smith, A.; Ooi, E. E.; Vasudevan, S. G.; Gubler, D. J. Curr Infect Dis Rep 2010, 12, 157–164.
36. Guy, B.; Almond, J.; Lang, J. Lancet 2011, 377, 381–382.
37. Stein, D. A.; Perry, S. T.; Buck, M. D.; Oehmen, C. S.; Fischer, M. A.; Poore, E.; Smith, J. L.; Lancaster, A. M.; Hirsch, A. J.; Slifka, M. K.; Nelson, J. A.; Shresta, S.; Früh, K. J Virol 2011, 85, 10154–10166.
38. Clemons, A.; Haugen, M.; Le, C.; Mori, A.; Tomchaney, M.; Severson, D. W.; Duman-Scheel, M. PLoS ONE 2011, 6(1), e16730 (6 pp).
39. Roy, A.; Kucukural, A.; Zhang, Y. Nat Protoc 2010, 5, 725–738.
40. Byrd, C. M.; Dai, D.; Grosenbach, D. W.; Berhanu, A.; Jones, K. F.; Cardwell, K. B.; Schneider, C.; Wineinger, K. A.; Page, J. M.; Harver, C.; Stavale, E.; Tyavanagimatt, S.; Stone, M. A.; Bartenschlager, R.; Scaturro, P.; Hruby, D. E.; Jordan, R. Antimicrob Agents Chemother 2013, 57, 15–25.
41. Schmidt, A. G.; Yang, P. L.; Harrison, S. C. PLoS Pathog 2010, 6(4), e1000851 (11 pp).
42. Tomlinson, S. M.; Malmstrom, R. D.; Watowich, S. J Infect Dis 2009, 9, 327–343.
43. Sievers, F.; Wilm, A.; Dineen, D.; Gibson, T. J.; Karplus, K.; Li, W.; Lopez, R.; McWilliam, H.; Remmert, M.; Söding, J.; Thompson, J. D.; Higgins, D. G. Mol Syst Biol 2011, 7, 539 (6 pp).
44. Walia, R. R.; Caragea, C.; Lewis, B. A.; Towfic, F.; Terribilini, M.; El-Manzalawy, Y.; Dobbs, D.; Honavar, V. BMC Bioinformatics 2012, 13, 89 (20 pp).
45. DeLano, W. The PyMOL Molecular Graphics System; DeLano Scientific LLC: Palo Alto, CA, 2008.
46. Klug, A.; Finch, J. T.; Franklin, R. E. Biochim Biophys Acta 1957, 25, 242–252.
47. Caspar, D. L.; Klug, A. Cold Spring Harbor Symp Quant Biol 1962, 27, 1–24.
48. Fromentin, R.; Majeau, N.; Laliberté Gagné, M.-E.; Boivin, A.; Duvignaud, J.-B.; Leclerc, D. Anal Biochem 2007, 366, 37–45.
49. Cadena-Nava, R. D.; Comas-Garcia, M.; Garmann, R. F.; Rao, A. L. N.; Knobler, C. M.; Gelbart, W. M. J Virol 2012, 86, 3318–3326.
50. Zhang, W.; Mukhopadhyay, S.; Pletnev, S. V.; Baker, T. S.; Kuhn, R. J.; Rossmann, M. G. J Virol 2002, 76, 11645–11658.
51. Carrillo-Tripp, M.; Shepherd, C. M.; Borelli, I. A.; Venkataraman, S.; Lander, G.; Natarajan, P.; Johnson, J. E.; Brooks, C. L.; Reddy, V. S. Nucleic Acids Res 2009, 37, D436–D442.
52. Paredes, A. M.; Brown, D. T.; Rothnagel, R.; Chiu, W.; Schoepp, R. J.; Johnston, R. E.; Prasad, B. V. Proc Natl Acad Sci USA 1993, 90, 9095–9099.
53. Cheng, R. H.; Kuhn, R. J.; Olson, N. H.; Rossmann, M. G.; Choi, H. K.; Smith, T. J.; Baker, T. S. Cell 1995, 80, 621–630.
54. Perera, R.; Kuhn, R. J. Curr Opin Microbiol 2008, 11, 369–377.
55. Wilkins, M. R.; Gasteiger, E.; Bairoch, A.; Sanchez, J. C.; Williams, K. L.; Appel, R. D.; Hochstrasser, D. F. Methods Mol Biol 1999, 112, 531–552.
56. Markoff, L.; Falgout, B.; Chang, A. Virology 1997, 233, 105–117.
57. Kaufmann, B.; Chipman, P. R.; Holdaway, H. A.; Johnson, S.; Fremont, D. H.; Kuhn, R. J.; Diamond, M. S.; Rossmann, M. G. PLoS Pathog 2009, 5(11), e1000672 (5 pp).
58. Strauss, J. H.; Strauss, E. G. Annu Rev Microbiol 1988, 42, 657–683.
59. Strauss, J. H.; Strauss, E. G. Cell 2001, 105, 5–8.
60. Helenius, A. Cell 1995, 81, 651–653.
61. Linger, B. R.; Kunovska, L.; Kuhn, R. J.; Golden, B. L. RNA 2004, 10, 128–138.
62. Martins, I. C.; Gomes Neto, F.; Faustino, A. F.; Carvalho, F. A.; Carneiro, F. A.; Bozza, P. T.; Mohana-Borges, R.; Castanho, M. A. R. B.; Almeida, F. C. L.; Santos, N. C.; Da Poian, A. T. Biochem J 2012, 444, 405–415.
63. Kiermayr, S.; Kofler, R. M.; Mandl, C. W.; Messner, P.; Heinz, F. X. J Virol 2004, 78, 8078–8084.
64. Hagan, M. F.; Chandler, D. Biophys J 2006, 91, 42–54.
65. Mukhopadhyay, S.; Chipman, P. R.; Hong, E. M.; Kuhn, R. J.; Rossmann, M. G. J Virol 2002, 76, 11128–11132.
66. Carpenter, M. L.; Oliver, A. W.; Kneale, G. G. Methods Mol Biol 2001, 148, 503–510.
67. Garbett, N. C.; Ragazzon, P. A.; Chaires, J. B. Nat Protoc 2007, 2, 3166–3172.
68. Johnston, I. G.; Louis, A. A.; Doye, J. P. K. J Phys: Condens Matter 2010, 22, 104101 (9 pp).
69. Luque, A.; Zandi, R.; Reguera, D. Proc Natl Acad Sci USA 2010, 107, 5323–5328.
70. Angelescu, D. G.; Linse, P. Soft Matter 2008, 4, 1981–1990.
71. Cheng, S.; Brooks, C. L., III. PLoS Comput Biol 2013, 9(2), e1002905.
72. Choi, H. K.; Lu, G.; Lee, S.; Wengler, G.; Rossmann, M. G. Proteins 1997, 27, 345–359.
73. Alves, C. S.; Melo, M. N.; Franquelim, H. G.; Ferre, R.; Planas, M.; Feliu, L.; Bardaji, E.; Kowalczyk, W.; Andreu, D.; Santos, N. C.; Fernandes, M. X.; Castanho, M. A. R. B. J Biol Chem 2010, 285, 27536–27544.
74. Freire, J. M.; Veiga, A. S.; de la Torre, B. G.; Andreu, D.; Castanho, M. A. R. B. J Pept Sci 2013, 19, 182–189.
75. Lakowicz, J. R. Principles of Fluorescence Spectroscopy, 2nd ed.; Kluwer Academic/Plenum Publishers: New York, NY, 1999.
76. Rohacova, J.; Marin, M. L.; Miranda, M. A. J Phys Chem B 2010, 114, 4710–4716.
77. Provencher, S. W. Comput Phys Commun 1982, 27, 213–227.
78. Provencher, S. W. Comput Phys Commun 1982, 27, 229–242.
79. Santos, N. C.; Castanho, M. A. Biophys J 1996, 71, 1641–1650.
80. Domingues, M. M.; Santiago, P. S.; Castanho, M. A. R. B.; Santos, N. C. J Pept Sci 2008, 14, 394–400.
81. Kelly, S. M.; Jess, T. J.; Price, N. C. Biochim Biophys Acta 2005, 1751, 119–139.
82. Louis-Jeune, C.; Andrade-Navarro, M. A.; Perez-Iratxeta, C. Proteins 2011, 80, 374–381.
83. Carpenter, M. L.; Kneale, G. G. Methods Mol Biol 1994, 30, 313–325.
84. Santos, N. C.; Castanho, M. A. R. B. Trends Appl Spectrosc 2002, 4, 113–125.